Computed Tomographic (CT) Reconstruction of the Average Propagator from Diffusion Weighted MR Data

W. R. Jarisch[1], E. Özarslan[2], and P. J. Basser[3]

[1]Cyber Technology, Potomac, MD, United States, [2]NICHD, NIH, Bethesda, MD, United States, [3]NICHD, NIH, Bethesda, MD

Introduction

K- and q-space MRI (1) is a classical method for measuring the *entire* average propagator, $P(\boldsymbol{r})$, in each voxel of an imaging volume using a 3-D Inverse Fourier Transform (IFT) of the diffusion weighted imaging (DWI) signal, $E(\boldsymbol{q})$. $P(\boldsymbol{r})$ provides key architectural and microstructural features in tissues without employing a parametric model of the diffusion process. The bottleneck in measuring $P(\boldsymbol{r})$ *in vivo*, however, is the large number of DWIs required. Our long-term goal is to measure $P(\boldsymbol{r})$ in its entirety in each voxel of an imaging volume using about 256 DWIs. To achieve this we 1) reformulate the estimation of $P(\boldsymbol{r})$ from DWI signals as a computed tomography (CT) reconstruction problem, 2) employ *a priori* information about properties of DWIs and $P(\boldsymbol{r})$ to constrain the CT reconstruction, and 3) use this reconstruction framework to optimize the experimental design.

Theory

The 3-D IFT relationship between $P(\boldsymbol{r})$ and $E(\boldsymbol{q})$ in each voxel is given below,

$$P(\boldsymbol{r}) = \iiint E(\boldsymbol{q}) e^{2\pi i \boldsymbol{q} \bullet \boldsymbol{r}} d\boldsymbol{q}^3 \qquad (1)$$

where the vector $\boldsymbol{r}$ is the net displacement of spin-labeled molecules, $E(\boldsymbol{q})$ is the complex-valued DW MR signal, and the vector $\boldsymbol{q}$ specifies the strength and direction of the diffusion sensitizing gradients. Brute-force, direct inversion of Eq. (1), using the 3-D IFFT, as in Diffusion Spectrum Imaging (DSI) (2), is too costly in scan time, in principle, requiring at least 8192 (=16x[16x32]) DWIs to determine $P(\boldsymbol{r})$ with high fidelity.

The form of Eq. (1) suggests that $P(\boldsymbol{r})$ is a 3-D density, and its planar projections are isomorphic to $E(\boldsymbol{q})$ slices via the Fourier slice theorem. In principle, we can then use CT reconstruction methods to estimate $P(\boldsymbol{r})$ from oblique $E(\boldsymbol{q})$ slices. The difference here is these CT reconstructions are performed within a single anatomical voxel within an imaging volume.

To reduce the number of DWI samples required and increase the accuracy of the tomographic reconstruction of $P(\boldsymbol{r})$ we apply physical constraints, such as: (i) $P(\boldsymbol{r}) \geq 0$; (ii) $P(\boldsymbol{r}) \geq P(\gamma\, \boldsymbol{r})\ \forall\ \gamma \geq 1$; (iii) $E(\boldsymbol{0}) \approx E(\delta\boldsymbol{q}) + \alpha\ \delta\boldsymbol{q}^{T}\ \mathbf{D}\ \delta\boldsymbol{q}$ for sufficiently small $|\delta\boldsymbol{q}|$, where $\mathbf{D}$ is the diffusion tensor obtained from DTI and $\alpha > 0$. Constraint (i) significantly reduces the space of possible solutions for $P(\boldsymbol{r})$; constraint (ii) requires that $P(\boldsymbol{r})$ declines monotonically; constraint (iii) reduces the number of $E(\boldsymbol{q})$ required at small $|\delta\boldsymbol{q}|$.

High-Efficiency CT (HECT) (3), a new CT reconstruction method based on an approximation to Bayes Maximum *a posteriori* (MAP) estimation (4), is used to calculate $P(\boldsymbol{r})$ from $E(\boldsymbol{q})$ data obtained on different oblique planes in q-space. Currently, HECT can accommodate constraint (i) above. Moreover, these plane projections may be noisy, the number of projections may be small (i.e., the inverse problem may be ill-posed), and arbitrary projection directions may be used.

Results

We implemented several simulations of hindered and restricted diffusion using synthetic NMR "phantoms" to test the accuracy, precision, robustness, noise immunity and speed of this CT reconstruction framework of $P(\boldsymbol{r})$. The original DWI data sets were generated with 8192 $E(\boldsymbol{q})$ data points having 16 oblique planes passing through $\boldsymbol{q}=\mathbf{0}$, each with 16x32 points, whose slopes coincide with the faces of a quasi-regular icosidodecahedron. The diffusion phantom shown in Fig 1a, was generated from a 3-compartment Gaussian displacement distribution. It was found that 2048 $E(\boldsymbol{q})$ sub-samples were sufficient to produce a 3D reconstruction of $P(\boldsymbol{r})$ with ~1% RMS error using only four plane projections (with q-planes arranged in a tetrahedral pattern). Fig 1b. and c. show iso-probability contours of the estimated $P(\boldsymbol{r})$ with a threshold set at 4% of the peak value, $P(\mathbf{0})$, without and with 4% RMS Rician noise, respectively. Note: currently, the HECT algorithm requires at least 32 pixels in each slice dimension. On a desktop PC, each complete $P(\boldsymbol{r})$ reconstruction takes approximately 1 second.

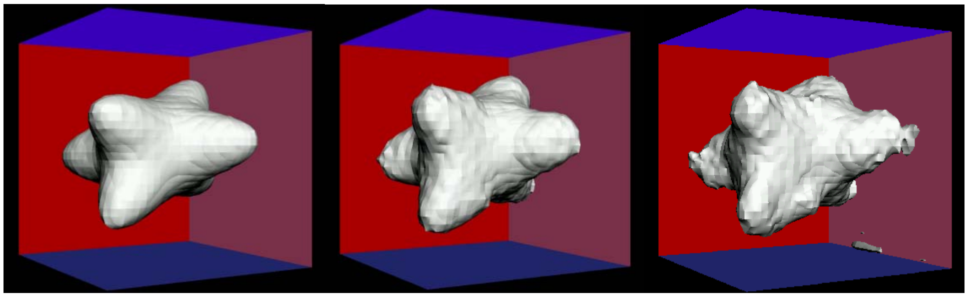

Figure 1: (a) Diffusion phantom iso-density contour at 4% of $P(\mathbf{0})$; (b) Four-view HECT without noise; (c) Four-view HECT with RMS Rician noise at 4% of $E(\mathbf{0})$.

Discussion and Conclusion

Preliminary results for the HECT reconstruction of $P(\boldsymbol{r})$ are encouraging. Algorithmic improvements should result in significant speedup and a four-fold reduction in the number of DWIs required from 2048 to 512 at half resolution. Further reductions in the DWI data required are expected through experimental design optimization, and by applying additional constraints and *a priori* information. Significant computational speedup is also possible using faster processors with multiple threads.

Bibliography

1. Callaghan PT *et al.*,. 1988. NMR microscopy of dynamic displacements: k-space and q-space imaging. J. Phys. E: Sci. Instrum. 21:820-822.
2. Wedeen VJ *et al.*, 2005. Mapping complex tissue architecture with diffusion spectrum magnetic resonance imaging. Magn Reson Med 54:1377-1386.
3. Jarisch WR, 2008. HECT - High Efficiency Computed Tomography, A Powerful New Technique for Quantitative Tomography. In Microscopy and Microanalysis, Albuquerque, NM. Late Braking Poster #16.
4. Sage AP and Melsa JL, 1971. The Kalman-Bucy Filter McGraw-Hill, New York.